Frequency-dependent effects of the Atlantic meridional overturning on the tropical Pacific Ocean

L. A. te Raa,[1,3] G. J. van Oldenborgh,[2] H. A. Dijkstra,[1] and S. Y. Philip[2]

Using the ECHAM5/MPI-OM model, we study the relation between the variations in the Atlantic meridional overturning circulation (AMOC) and both the Pacific sea surface temperature (SST) and the El Niño-Southern Oscillation (ENSO) amplitude. In a 17-member 20C3M/SRES-A1b ensemble for 1950-2100 the Pacific response to AMOC variations associated with the Atlantic Multidecadal Oscillation (AMO) is very small. In a 5-member hosing ensemble where the AMOC collapses due to a large freshwater anomaly, the Pacific response is large and in correspondence with previous work. Our results show that the modeled connection between AMOC and ENSO depends very strongly on the frequency and/or the amplitude of the AMOC variations. Interannual AMOC variations, decadal AMOC variations and an AMOC collapse are associated with entirely different responses in the Pacific Ocean.

1. Introduction

Decadal to multidecadal modulations of the amplitude of ENSO have been found in observations of SST, sea level pressure and rainfall [e.g., Torrence and Webster, 1999]. Recently, multidecadal SST variations associated with the AMO have been suggested as a possible explanation for low-frequency ENSO variability [Dong et al., 2006; Timmermann et al., 2007]. The large-scale SST pattern of the AMO in the North Atlantic is thought to be related to multidecadal variations of the AMOC [Delworth and Mann, 2000; Knight et al., 2005; Dijkstra et al., 2006]. In particular, a positive AMO (relatively high North Atlantic SSTs) has been found to be associated with a strong AMOC [Knight et al., 2005], possibly with a phase lag between the maximum AMO and the maximum AMOC [Dijkstra et al., 2006]. Using a coupled ocean-atmosphere GCM, Dong et al. [2006] suggest that latent heat anomalies associated with a positive phase of the AMO lead to a deeper equatorial thermocline in the Pacific through anomalous easterly winds. This in turn reduces ENSO variance in the model. Sutton et al. [2007] also show that large-scale temperature anomalies in the North Atlantic Ocean can affect the tropical Pacific region.

Modeling studies in which a substantial weakening of the AMOC is induced by large freshwater anomalies indicate that changes in the AMOC can affect the tropical Pacific mean state, as well as ENSO amplitudes [Vellinga and Wood, 2002; Zhang and Delworth, 2005; Timmermann et al., 2005, 2007]. Timmermann et al. [2005] show that

a deepening of the equatorial thermocline in the eastern equatorial Pacific is brought about by oceanic waves after a collapse of the AMOC. Zhang and Delworth [2005] show that cooling in the tropical Atlantic results in a southward shift of the ITCZ, leading to upwelling and thus cooling (downwelling and thus warming) north (south) of the equator in the tropical eastern Pacific. A similar atmospheric bridge was found by Timmermann et al. [2007] in five coupled ocean-atmosphere GCMs. Although a collapse of the AMOC is unlikely in the near future, these results are considered to be of use in the current climate as an indication of the effects of natural variability of the AMOC, such as those associated with the AMO. However, the AMOC variations related to natural climate variability are much smaller than the 50-80% reduction typically induced by large freshwater anomalies.

In this paper, we compare the effect of AMOC changes on the tropical Pacific SST and ENSO amplitude using two ensembles of runs performed with the coupled ECHAM5/MPI-OM model. Using a 17-member ensemble of climate runs for the period 1950-2100 under the 20C3M/SRES-A1b scenario, we first study the response of the tropical Pacific to AMO variations. Next, the tropical Pacific response to a forced collapse of the AMOC is investigated in a 5-member ensemble performed with the same model for the period 2000-2100.

2. Model and numerical simulations

All experiments are part of the ESSENCE project (www.knmi.nl/~sterl/Essence) and have been conducted with the ECHAM5/MPI-OM coupled climate model, which is described by Roeckner et al. [2003] and Marsland et al. [2003]. Although the model suffers from a too pronounced and too far westward extending Pacific equatorial cold tongue, the simulated ENSO as well as the thermohaline circulation are quite reasonable [Marsland et al., 2003; Keenlyside et al., 2005; van Oldenborgh et al., 2005]. The model is run in the configuration used for the AR4 climate scenario runs, with a horizontal resolution of T63 and 21 vertical hybrid levels in the atmosphere and an average horizontal resolution of 1.5° and 40 vertical layers in the ocean.

The standard ensemble consists of 17 runs over the period 1950-2100. Greenhouse gas and tropospheric aerosol concentrations are specified from observations for 1950-2000 and follow the SRES-A1b scenario for 2001-2100. The runs are initialized from the year 1950 of a 20th century simulation, with the atmospheric temperature perturbed by adding Gaussian noise with an 0.1°C amplitude. The hosing ensemble consists of 5 members, each initialized from the year 2000 from a different member of the standard ensemble. A 1 Sv freshwater anomaly was added in an area near Greenland from the end of year 2000 onwards. Apart from this additional freshwater input, the forcing is the same as in the standard ensemble.

3. Results

The AMO index, calculated as the average of monthly SST anomalies with respect to the ensemble mean over the North Atlantic north of 25°N (75°W-7°W , 25°N-60°N),

---

[1]Institute for Marine and Atmospheric research Utrecht, Utrecht University, Netherlands

[2]Royal Netherlands Institute of Meteorology, De Bilt, Netherlands

[3]Currently at Netherlands Organisation for Applied Scientific Research TNO, The Hague, Netherlands
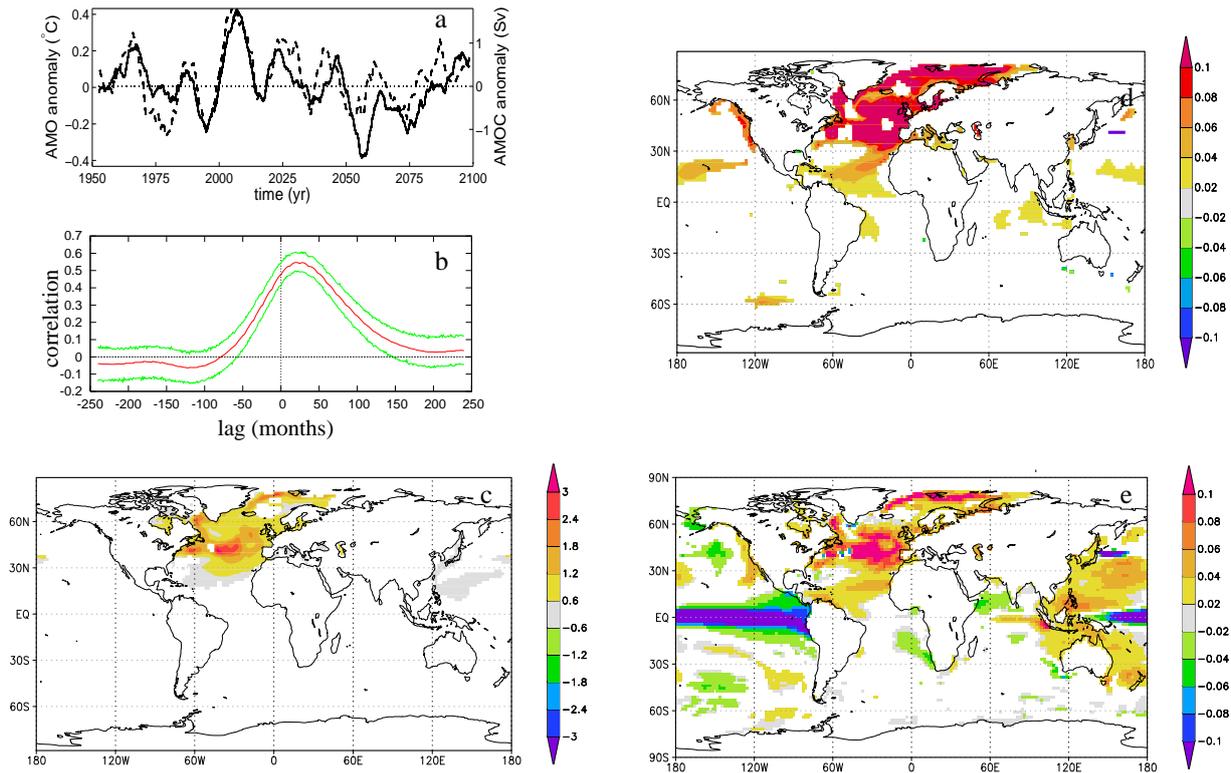
Figure 1. (a) AMO index (solid) and maximum AMOC at 35°N (dashed) for standard ensemble member 4. (b) Lag correlation between maximum AMOC at 35°N and the AMO index. For positive lags the AMOC is leading. The green band indicates the 95% confidence interval based on a decorrelation time scale of 5 years. (c) Regression (°C/°C) of SST on the AMO index. (d) Regression (°C/Sv) of SST on maximum AMOC at 35°N. (e) Regression (°C/Sv) of annual mean SST on annual mean maximum AMOC at 35°N. Unless stated otherwise, in all panels data are 5-yr running means of anomalies with respect to the ensemble mean. In (b)-(e), data of all standard ensemble members have been used. Areas in (c)-(e) for which the p-value exceeds 10% in a two-sided t-test are not shaded.

shows variations of -0.4 °C to 0.4 °C in individual members of the standard ensemble (Fig. 1a). These amplitudes are in reasonable agreement with observations [Enfield et al., 2001; Knight et al., 2005; Sutton and Hodson, 2005]. The maximum AMOC at 35°N varies about 1 Sv around the ensemble mean (Fig. 1a). The average period of the multi-decadal variability in AMO and AMOC is about 20 years. Although shorter than observed, this is very similar to what was found by Dong and Sutton [2005] in the HadCM3 model. The correlation between the AMO index and the AMOC for all standard ensemble members together is 0.55, with the overturning leading by about 2 years (Fig. 1b). Hence there is a significant relation between the AMO and the multi-decadal AMOC variability in this model. The fact that the AMO index lags the maximum AMOC is in agreement with the mechanism of the AMO as suggested in Te Raa and Dijkstra [2002].

There is no statistically significant response of tropical Pacific SST to the AMO (Fig. 1c). Note that by using only SSTs north of 25°N in the AMO index, the inclusion of tropical Atlantic ENSO teleconnections (that could cloud the AMOC-related variability the AMO index is thought to express) is avoided. The correlation between 5-yr running means of the AMO and the Niño3.4 index is less than 0.22 for any lag varying from 0 to 20 years (AMO leading). To study the relation between Pacific SST and the AMOC directly, we also computed the correlation between 5-yr running means of the Niño3.4 index and the maximum AMOC at 35°N. These correlations are even lower, with maxima less than 0.1 for lags with the AMOC leading. The SST response to AMOC variations is indeed mostly confined to the North Atlantic (Fig. 1d), with no significant correlations in the equatorial Pacific.

In contrast, higher-frequency variability of the AMOC is strongly correlated with ENSO. The regression of SST on maximum AMOC at 35°N without application of a running mean seems to yield a clear response in the equatorial Pacific (Fig. 1e). However, the apparent correlation between the AMOC and tropical Pacific SSTs turns out to be caused by the NAO projecting on both of them: the correlation between annual mean values of the NAO and Niño3.4 indices is 0.35, and between the NAO index and the maximum AMOC at 35°N -0.33. An NAO that is driven by ENSO is a common model artifact: in the observations the two are uncorrelated (a typical correlation coefficient over 1851-2005 is 0.01).

Having found no significant correlation between decadal AMOC variability and the mean temperature of the ENSO region, we turn to ENSO amplitudes. The lagged correlation between a 15-yr running standard deviation of Niño3.4 and the 5-yr running mean of maximum AMOC at 35°N is at most -0.2 with the AMOC leading (not shown). A similar correlation with the AMO index is not statistically significant at the 95% level for any lag up to 20 years (AMO leading). From these results we conclude that in the standard ensemble, the AMO-related AMOC variability has no significant effects on ENSO amplitudes either.

In the hosing ensemble, the AMOC collapses to about 3 Sv in the year 2100 (Fig. 2a). As the AMOC also decreases in the standard ensemble (Fig. 2a), and greenhouse gases are taken from the A1b scenario in the hosing runs, we compute the effect of AMOC decrease induced by the freshwater anomaly itself as the regression of the difference of hosing and standard runs with respect to the difference in
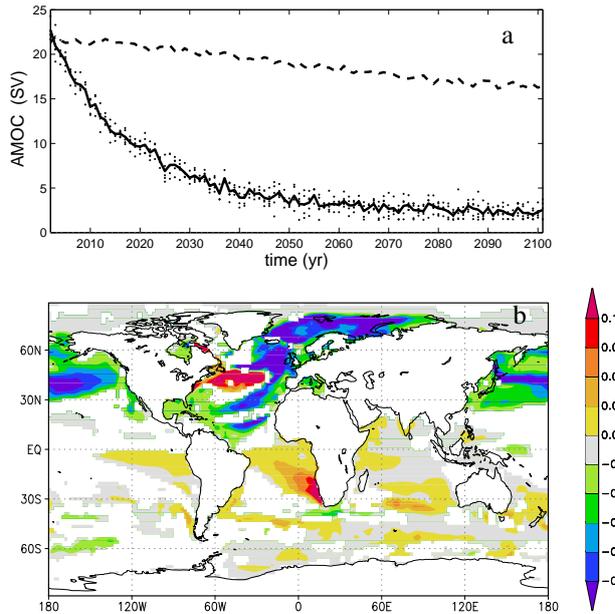
Figure 2. (a) Maximum AMOC at $35°$N (Sv) of all hosing ensemble members, together with their ensemble mean (solid). The standard ensemble mean (dashed) is given for comparison. (b) Regression of the difference in SST between the hosing and standard runs on the difference in maximum AMOC at $35°$N ($°$C/Sv) for 2000-2050. A 5-yr running mean has been applied to the data before regressing. Shading as in Fig. 1.

AMOC strengths, i.e., the regression of $T_{\text{hosing}} - T_{\text{stand}}$ on $\Psi^{\text{max}}_{\text{hosing}} - \Psi^{\text{max}}_{\text{stand}}$. In general, the strongest response is found on the northern hemisphere (Fig. 2b). With statistically significant regression coefficients exceeding $0.03°$C/Sv there is also a clear response in the equatorial Pacific SST. The response of global SST (and of the tropical Pacific SST in particular) in the hosing ensemble is thus very different from that in the standard ensemble (compare Figs 1d and 2b).

In the hosing ensemble, it takes about 10 years after the start of the freshwater anomaly before a significant change in SST in the tropical Pacific occurs (Fig. 3a). In fact, cooling only reaches the tropical Pacific after having reached the Caribbean (Fig. 3b). Except for this time delay, the response is completely linear. Once the temperature in the Caribbean starts to drop, an atmospheric anticyclone develops over this region (not shown), and the easterly trade winds over central America intensify (Fig. 3c), thereby cooling the equatorial Pacific.

The spatial pattern of the regression of zonal wind stress on AMOC variations indeed shows a strong and localized response over Central America (Fig. 4a). This atmospheric bridge is in agreement with results of Timmermann et al. [2007] and Dong and Sutton [2007] and has been described in detail by Zhang and Delworth [2005] and Xie et al. [2007]. However, the spatial pattern of the zonal wind stress response to AMOC changes associated with the AMO is crucially different (Fig. 4b) from that in Fig. 4a as there is no signature of an atmospheric bridge connecting the Atlantic and Pacific Oceans.

4. Discussion and Conclusion

Our results show that a weakening of the AMOC induced by a large freshwater anomaly generates a different response of Pacific SST than that due to the AMO variability. There are two possibilities to explain the lack of the Pacific SST response to AMO variability in this model. The first explanation is that the time scale of the multidecadal variability in the standard ensemble is too short to cause sufficiently strong SST anomalies in the Caribbean. Then also zonal wind anomalies do not have enough time to develop before the AMOC anomaly changes sign, and consequently no signal is transmitted to the equatorial Pacific. The second explanation is that the amplitude and/or spatial pattern of the SST response generated by the AMO are such that the Caribbean SST hardly changes, and thus no signal is transmitted to the Pacific. In fact, Figs 3b and 3c even suggest that the response of Caribbean temperature and Central American wind stress to AMOC variations might be nonlinear, with a critical threshold of AMOC variations below which no response in the Pacific occurs, and a linear response above this. The amplitude dependence could be tested with the data of Stouffer et al. [2006], which reports on 0.1 Sv and 1 Sv hosing experiments but did not investigate the linearity of teleconnections.

The implications of these results are twofold. Firstly, the different response of tropical Pacific SSTs to AMOC variations associated with the AMO and an AMOC collapse means that results from experiments with a collapsed AMOC [Vellinga and Wood, 2002; Zhang and Delworth, 2005; Timmermann et al., 2005, 2007] can not be extrapolated to the natural variability in the current model. Secondly, the response of tropical Pacific SSTs to an imposed
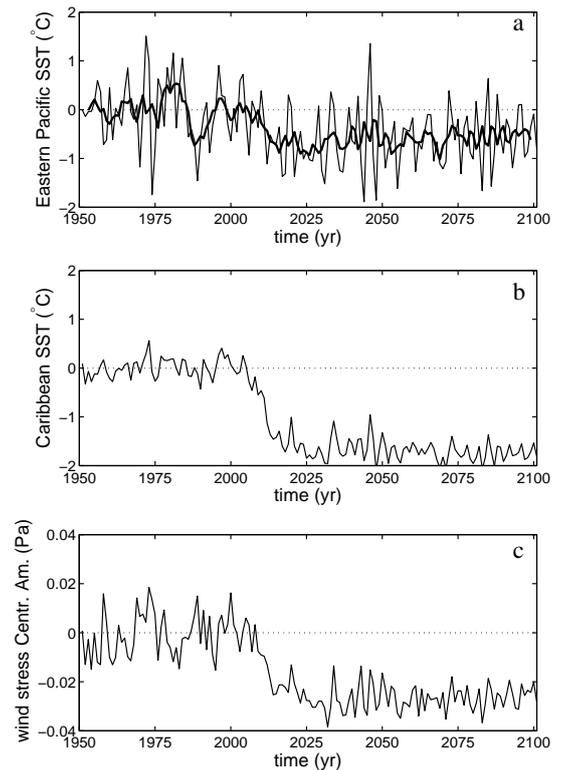
Figure 3. Difference between ensemble mean values of hosing and standard ensembles (for 2001-2100). For 1950-2000, the difference between standard member 2 and the ensemble mean of the standard ensemble is shown. (a) Annual mean SST ($°$C, thin line) and 5-yr running means (thick line) averaged over the eastern Pacific ($150°$W-$90°$W, $10°$S-$10°$N). (b) Annual mean SST ($°$C) averaged over the Caribbean ($90°$W-$60°$W, $10°$N-$20°$N). (c) Annual mean zonal wind stress (Pa) averaged over Central America ($100°$W-$75°$W, $5°$N-$20°$N).

AMO-like spatial SST pattern [Dong et al., 2006; Sutton et al., 2007] is most likely very sensitive to the amplitude of this AMO pattern in the Caribbean.

In summary, our results indicate that the relation between AMOC variations and Pacific SST is frequency and/or amplitude dependent. Further study will be needed to investigate why the Pacific SST response to AMO variability in this model is so weak. To test the explanation that the time scale of the multidecadal variability in the current model is responsible for the lack of response, the relation between AMOC variability and equatorial Pacific SST will have to be investigated in a run with multidecadal variations on time scales longer than 20 years. Furthermore, runs with different strength of freshwater anomalies will be needed to test if threshold behavior of Caribbean SST exists.

References

Delworth, T. L. and M. E. Mann, 2000: Observed and simulated multidecadal variability in the Northern Hemisphere. *Clim. Dyn.*, **16**, 661–676.

Dijkstra, H. A., L. A. Te Raa, M. Schmeits, and J. Gerrits, 2006: On the physics of the Atlantic Multidecadal Oscillation. *Ocean Dynamics*, **56**, 36–50.

Dong, B. and R. T. Sutton, 2005: Mechanism of interdecadal thermohaline circulation variability in a coupled ocean–atmosphere GCM. *J. Climate*, **18**, 1117–1135.

— 2007: Enhancement of ENSO variability by a weakened Atlantic thermohaline circulation in a coupled GCM. *J. Climate*, **20**, 4920–4939.

Dong, B., R. T. Sutton, and A. A. Scaife, 2006: Multidecadal modulation of El Niño-Southern Oscillation (ENSO) variance by Atlantic Ocean sea surface temperatures. *Geophys. Res. Lett.*, **33**.

Enfield, D. B., A. M. Mestas-Nuñe, and P. Trimble, 2001: The Atlantic Multidecadal Oscillation and its relation to rainfall and river flows in the continental U.S. *Geophys. Res. Lett.*, **28**, 2077–2080.

Keenlyside, N., M. Latif, M. Botzet, J. Jungclaus, and U. Schulzweida, 2005: A coupled method for initializing El Niño Southern Oscillation forecasts using sea surface temperature. *Tellus*, **A57**, 340, doi:10.1111/j.1600-0870.2005.00107.x.

Knight, J. R., R. J. Allan, c. K. Folland, M. Vellinga, and M. E. Mann, 2005: A signature of persistent natural thermohaline circulation cycles in observed climate. *Geophys. Res. Lett.*, **32**.

Marsland, S. J., H. Haak, J. H. Jungclaus, M. Latif, and F. Röske, 2003: The Max-Planck-Institute global ocean/sea ice model with orthogonal curvilinear coordinates. *Ocean Modelling*, **5**, 91–127.

Roeckner, E., G. Bäuml, L. Bonaventura, R. Brokopf, M. Esch, M. Giorgetta, S. Hagemann, I. Kirchner, L. Kornblueh, E. Manzini, A. Rhodin, U. Schlese, U. Schulzweida, and A. Tompkins, 2003: The atmospheric general circulation model ECHAM 5. Part I: Model description. Technical Report 349, Max-Planck-Institut für Meteorologie, Hamburg, Germany.

Stouffer, R. J. et al., 2006: Investigating the causes of the response of the thermohaline circulation to past and future climate changes. *J. Climate*, **19**, 1365–1387.

Sutton, R. T., B.-W. Dong, and J. M. Gregory, 2007: Land/sea warming ratio in response to climate change: IPCC AR4 model results and comparison with observations. *Geophys. Res. Lett.*, **34**, L02701, doi:10.1029/2006GL028164.

Sutton, R. T. and D. L. R. Hodson, 2005: Atlantic Ocean forcing of North American and European summer climate. *Science*, **309**, 115–118.

Te Raa, L. A. and H. A. Dijkstra, 2002: Instability of the thermohaline ocean circulation on interdecadal time scales. *J. Phys. Oc.*, **32**, 138–160.

Timmermann, A., S.-I. An, U. Krebs, and H. Goosse, 2005: ENSO suppression due to weakening of the North Atlantic thermohaline circulation. *J. Climate*, **18**, 3122–3139.

Timmermann, A., Y. Okumura, S. I. An, A. Clement, B. Dong, E. Guilyardi, A. Hu, J. H. Jungclaus, M. Renold, T. F. Stocker, R. J. Stouffer, R. T. Sutton, S. P. Xie, and J. Yin, 2007: The influence of a weakening of the Atlantic meridional overturning circulation on ENSO. *J. Climate*, **20**, 4899–4918.

Torrence, C. and P. J. Webster, 1999: Interdecadal changes in the ENSO-monsoon system. *J. Climate*, **12**, 2679–2690.

van Oldenborgh, G. J., S. Y. Philip, and M. Collins, 2005: El Niño in a changing climate: a multi-model study. *Ocean Science*, **1**, 81–95.

Vellinga, M. and R. Wood, 2002: Global climatic impacts of a collapse of the Atlantic thermohaline circulation. *Climatic Change*, **54**, 251–267.

Xie, S.-P., T. Miyama, Y. Wang, H. Xu, S. P. De Szoeke, R. J. O. Small, K. J. Richards, T. Mochiziku, and T. Awaji, 2007: A regional ocean-atmosphere model for eastern Pacific climate: toward reducing tropical biases. *J. Climate*, **20**.

Zhang, R. and T. L. Delworth, 2005: Simulated tropical response to a substantial weakening of the Atlantic thermohaline circulation. *J. Climate*, **18**, 1853–1860.

G. J. van Oldenborgh, Royal Netherlands Institute of Meteorology, P. O. Box 201, 3730 AE De Bilt, Netherlands (oldenborgh@knmi.nl).
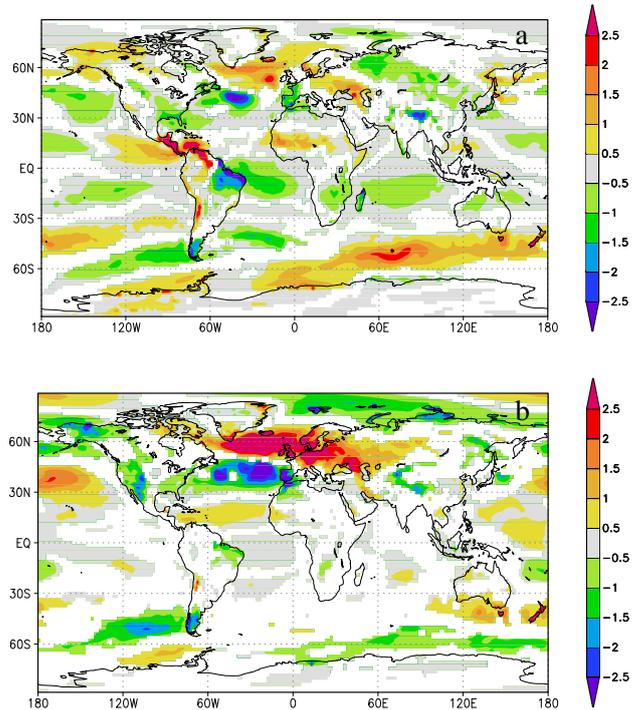
Figure 4. (a) Regression of the difference in zonal wind stress between the hosing and standard ensembles on the difference in maximum AMOC at $35°$N (10^{-3} Pa/Sv). (b) Regression of anomalies (w.r.t. the ensemble mean) of zonal wind stress on maximum AMOC at $35°$N (10^{-3} Pa/Sv) for all standard ensemble members. In both panels a 5-yr running mean has been applied to the data before regressing. Shading as in Fig. 1.